PHYSICAL REVIEW D **87,** 094004 (2013)

Exclusive decay of Υ into $J/\psi + \chi_{c0,1,2}$

Jia Xu,[1,*] Hai-Rong Dong,[1,†] Feng Feng,[2,‡] Ying-Jia Gao,[3,§] and Yu Jia[1,4,‖]

[1]*Institute of High Energy Physics, Chinese Academy of Sciences, Beijing 100049, China*
[2]*Center for High Energy Physics, Peking University, Beijing 100871, China*
[3]*Key Laboratory of Frontiers in Theoretical Physics, Institute of Theoretical Physics, Chinese Academy of Sciences, Beijing 100190, China*
[4]*Theoretical Physics Center for Science Facilities, Chinese Academy of Sciences, Beijing 100049, China*

(Received 17 December 2012; published 6 May 2013)

We study the Υ exclusive decay into double charmonium, specifically, the S-wave charmonium J/ψ plus the P-wave charmonium $\chi_{c0,1,2}$ in the nonrelativistic QCD factorization framework. Three distinct decay mechanisms, i.e., the strong, electromagnetic, and radiative decay channels, are included, and their interference effects are investigated. The decay processes $\Upsilon(1S, 2S, 3S) \to J/\psi + \chi_{c1,0}$ are predicted to have the branching fractions of order 10^{-6}, which should be observed in the prospective Super B factory.

DOI: 10.1103/PhysRevD.87.094004 PACS numbers: 12.38.−t, 12.38.Bx, 13.25.Gv

I. INTRODUCTION

Anyone who has ever browsed the meson summary table in the biannual review of Particle Data Group will be impressed by the extremely rich decay channels of the B, D, and J/ψ mesons [1]. Unlike the heavy flavored mesons, which can only decay via the weak interaction, the unflavored heavy quarkonia decay through the heavy quark-antiquark annihilation initiated exclusively by the strong and electromagnetic interactions. Although quite a few decay channels have been established for the charmonia system over the past few decades, the experimental information about the bottomonia decay is still very sparse. Very recently, however, the BELLE Collaboration observed a few exclusive decay channels of $\Upsilon(1S, 2S)$ into light hadrons for the first time, e.g., into the vector-tensor states and the axial-vector-pseudoscalar states [2].

Because of the much more copious phase space opened at the bottomonium energy level, the typical branching fraction for a given hadronic decay mode of a bottomonium is greatly diluted with respect to that of a charmonium. Thanks to the weaker strong coupling at the bottom mass scale, the perturbative QCD is expected to work more reliably for the hadronic bottomonium decay than for the charmonium.

An interesting class of hadronic decay processes is that of bottomonium into double charmonium, which may be predicted with fewer uncertainties than those into the light hadrons. In the recent years, some exclusive decay processes of bottomonium into double charmonia have been intensively studied in the perturbative QCD framework, e.g., $\eta_b \to J/\psi J/\psi$ [3–6], $\chi_{b0,1,2} \to J/\psi J/\psi$ [7–11], and $\Upsilon \to J/\psi + \eta_c$ [12,13]. These studies are largely inspired by the various double-charmonium production processes in e^+e^- annihilation, which were first observed at the B factories a decade ago [14–16]. Triggered by the disquieting discrepancy between data and theory, a great number of theoretical studies have since been conducted for the processes $e^+e^- \to J/\psi + \eta_c$ [17–29] and $e^+e^- \to J/\psi + \chi_{c0,1,2}$ [30–32].

Besides the tremendous amount of data near the $\Upsilon(4S)$, the BELLE experiment to date has also collected about 102 million $\Upsilon(1S)$ samples and 158 million $\Upsilon(2S)$ samples. Therefore, it appears more promising to observe the double-charmonium production from the Υ decay than from the C-even bottomonia decay. In Ref. [13], the exclusive decay of Υ to the vector-pseudoscalar charmonium states was studied in the framework of nonrelativistic QCD (NRQCD) factorization [33]. The corresponding branching fraction was estimated to be of order 10^{-6} and seems to have a good chance to be observed at the Super B factory. In this work, we further investigate the Υ decay into the J/ψ plus a spin-triplet P-wave charmonium χ_{cJ} ($J = 0, 1, 2$). This work should be considered as a sequel to Ref. [13].[1]

Although neither of these exclusive decay modes has been observed yet, several upper bounds for $\Upsilon(nS)$ inclusive decay into J/ψ or χ_{cJ} have already been placed experimentally [1], including

*xuj@ihep.ac.cn
†donghr@ihep.ac.cn
‡fengf@ihep.ac.cn
§josiagyj@hotmail.com
‖jiay@ihep.ac.cn

[1]The main results of this paper have already been reported in Ref. [34]. Nevertheless, some significant improvements have been made in the current work, i.e., some errors in calculating the three-gluon channel in Ref. [34] have been corrected, and the contribution from the two-gluon–one-photon channel is also included.

$$\begin{aligned}
&\mathcal{B}[\Upsilon(1S) \to J/\psi + X] = (6.5 \pm 0.7) \times 10^{-4},\\
&\mathcal{B}[\Upsilon(1S) \to \chi_{c0} + X] < 5 \times 10^{-3},\\
&\mathcal{B}[\Upsilon(1S) \to \chi_{c1} + X] = (2.3 \pm 0.7) \times 10^{-4},\\
&\mathcal{B}[\Upsilon(1S) \to \chi_{c2} + X] = (3.4 \pm 1.0) \times 10^{-4}\\
&\mathcal{B}[\Upsilon(2S) \to J/\psi + X] < 6 \times 10^{-3},\\
&\mathcal{B}[\Upsilon(4S) \to J/\psi + X] < 1.9 \times 10^{-4}.
\end{aligned} \tag{1}$$

It will be interesting to examine to what extent these upper bounds are saturated by the predicted branching fractions for $\Upsilon(nS) \to J/\psi + \chi_{c0,1,2}$.

As is well known, the hadronic decay of Υ can be categorized into three distinct classes—$b\bar{b}$ annihilating into three gluons (strong decay), a single photon (electromagnetic decay), or two-gluons and a photon (radiative decay). On experimental grounds, the following inclusive decay rates from these three decay channels have been available for a long time [1]:

$$\begin{aligned}
&\mathcal{B}[\Upsilon \to ggg]:\mathcal{B}[\Upsilon \to \gamma^* \to X]:\mathcal{B}[\Upsilon \to gg\gamma]\\
&\quad = 82.7\%:7.5\%:2.2\%,
\end{aligned} \tag{2}$$

where these three branching ratios sum up to $1 - \sum \mathcal{B}[\Upsilon \to l^+ l^-] = 92.5\%$, as they should.[2]

For the exclusive hadronic decay $\Upsilon \to J/\psi + \chi_{c0,1,2}$, one may also be interested in ascertaining the relative strength and the interference pattern among these different decay channels. This sort of study has been conducted for the process $\Upsilon \to J/\psi + \eta_c$ [13]. Note that there have lasted constant experimental efforts to infer the relative phase between the strong and electromagnetic amplitudes in exclusive J/ψ and ψ' decays into two light mesons [35–40]. As we will see later, as a consequence of $m_b > m_c \gg \Lambda_{\rm QCD}$, the relative phases among three distinct decay channels in our processes stem from the short-distance loop contribution, which can actually be calculated in perturbation theory.

The rest of the paper is organized as follows. In Sec. II, we express the polarized and unpolarized decay rates in terms of the helicity amplitudes and briefly state the helicity selection rule. In Sec. III, we conduct the lowest order (LO) calculation for each independent helicity amplitude associated with the decays $\Upsilon \to J/\psi + \chi_{c0,1,2}$, within the NRQCD factorization approach. The contributions from three distinct decay channels, i.e., electromagnetic, strong, and radiative decay channels, are all included, and the analytic expressions for each of the helicity amplitudes are given. In Sec. IV, we present our predictions of the interference pattern among three distinct decay channels for $\Upsilon \to J/\psi + \chi_{c0,1,2}$, and of the polarized and unpolarized partial decay widths and the corresponding branching fractions for $\Upsilon(1S, 2S, 3S)$ decays into $J/\psi + \chi_{c0,1,2}$. We find that it appears quite promising for the prospective Super B experiment to observe these hadronic decay processes. Finally, we summarize in Sec. V. In the Appendix, we list the explicit expressions of the 10 helicity projectors that are used in Sec. III.

[2]We have not included the contribution from the radiative transition $\Upsilon \to \eta_b \gamma$, which has a completely negligible branching ratio.

II. POLARIZED DECAY RATES AND HELICITY SELECTION RULE

It is of some advantage to utilize the helicity amplitude formalism [41,42] to analyze the hard exclusive reactions, in particular for the decay process studied in this work. From the experimental perspective, the helicity amplitudes can in principle be accessed by measuring the angular distributions of the decay products of J/ψ and χ_{cJ} ($J = 0, 1, 2$), provided that the statistics are sufficient. From the theoretical viewpoint, some essential dynamics underlying perturbative QCD is clearly encoded in the helicity amplitude analysis, which becomes rather obscured if one only looks at the unpolarized reaction rates.

We will work in the Υ rest frame throughout this work. Suppose the spin projection of the Υ along the $\hat{z}$ axis to be S_z (The $\hat{z}$ axis, for example, may be chosen as the beam direction of the e^- and e^+ collider, which resonantly produces a Υ meson). Let λ, $\tilde{\lambda}$ denote the helicities carried by the outgoing J/ψ and χ_{cJ}, respectively, and θ signify the angle between the J/ψ momentum $\mathbf{P}$ and the $\hat{z}$ axis. The differential polarized decay rate can be expressed as [41,42]

$$\begin{aligned}
&\frac{d\Gamma[\Upsilon(S_z) \to J/\psi(\lambda) + \chi_{cJ}(\tilde{\lambda})]}{d\cos\theta}\\
&\quad = \frac{|\mathbf{P}|}{16\pi M_\Upsilon^2} |d^1_{S_z,\lambda-\tilde{\lambda}}(\theta)|^2 |\mathcal{A}^J_{\lambda,\tilde{\lambda}}|^2,
\end{aligned} \tag{3}$$

where $\mathcal{A}^J_{\lambda,\tilde{\lambda}}$ ($J = 0, 1, 2$) characterizes the corresponding helicity amplitude, which encompasses all the nontrivial QCD dynamics. The angular distribution is fully dictated by the quantum numbers S_z, λ, and $\tilde{\lambda}$ through the Wigner rotation matrix $d^j_{m,m'}(\theta)$. Note that angular momentum conservation constrains that $|\lambda - \tilde{\lambda}| \le 1$. In (3), the magnitude of the three-momentum carried by the J/ψ (or χ_{cJ}) is determined by

$$|\mathbf{P}| = \frac{\lambda^{1/2}(M_\Upsilon^2, M_{J/\psi}^2, M_{\chi_{cJ}}^2)}{2M_\Upsilon}, \tag{4}$$

where $\lambda(x, y, z) = x^2 + y^2 + z^2 - 2xy - 2yz - 2zx$.

Integrating (3) over the polar angle, and averaging over all three possible Υ polarizations, one finds the integrated rate of Υ decay into $J/\psi + \chi_{cJ}$ in the helicity configuration $(\lambda, \tilde{\lambda})$ to be

$$\Gamma[\Upsilon \to J/\psi(\lambda) + \chi_{cJ}(\tilde{\lambda})] = \frac{|\mathbf{P}|}{16\pi M_\Upsilon^2} |\mathcal{A}^J_{\lambda,\tilde{\lambda}}|^2 \int_{-1}^{1} d\cos\theta \frac{1}{3} \sum_{S_z} |d^1_{S_z,\lambda-\tilde{\lambda}}(\theta)|^2 = \frac{|\mathbf{P}|}{24\pi M_\Upsilon^2} |\mathcal{A}^J_{\lambda,\tilde{\lambda}}|^2. \quad (5)$$

Since this decay process can be initiated by the strong or electromagnetic interactions, one can resort to the parity invariance to reduce the number of independent helicity amplitudes,

$$\mathcal{A}^J_{\lambda,\tilde{\lambda}} = (-1)^J \mathcal{A}^J_{-\lambda,-\tilde{\lambda}}. \quad (6)$$

As a consequence, the helicity channel $\Upsilon \to J/\psi(0) + \chi_{c1}(0)$ is strictly forbidden.

Starting from (5), one readily obtains the unpolarized decay rate by summing the contributions from all the allowed helicity channels,

$$\Gamma[\Upsilon \to J/\psi + \chi_{c0}] = \frac{|\mathbf{P}|}{24\pi M_\Upsilon^2} (|\mathcal{A}^0_{0,0}|^2 + 2|\mathcal{A}^0_{1,0}|^2), \quad (7a)$$

$$\Gamma[\Upsilon \to J/\psi + \chi_{c1}] = \frac{|\mathbf{P}|}{24\pi M_\Upsilon^2} (2|\mathcal{A}^1_{1,0}|^2 + 2|\mathcal{A}^1_{0,1}|^2 + 2|\mathcal{A}^1_{1,1}|^2), \quad (7b)$$

$$\Gamma[\Upsilon \to J/\psi + \chi_{c2}] = \frac{|\mathbf{P}|}{24\pi M_\Upsilon^2} (|\mathcal{A}^2_{0,0}|^2 + 2|\mathcal{A}^2_{1,0}|^2 + 2|\mathcal{A}^2_{0,1}|^2 + 2|\mathcal{A}^2_{1,1}|^2 + 2|\mathcal{A}^2_{1,2}|^2). \quad (7c)$$

There are two, three, and five independent helicity amplitudes for $\Upsilon \to J/\psi + \chi_{cJ}$ ($J = 0, 1, 2$), respectively, as enforced by the angular momentum conservation. We have also included a factor of 2 to account for the parity-doublet contributions.

One important piece of physics underlying the hard exclusive reactions is that each helicity amplitude possesses a definite power-law scaling in the inverse power of large momentum transfer, controlled by the helicity selection rule (HSR) [43]. At asymptotically large m_b, the polarized decay rate in our process scales as [17]

$$\frac{\Gamma[\Upsilon \to J/\psi(\lambda) + \chi_{cJ}(\tilde{\lambda})]}{\Gamma[\Upsilon \to \mu^+\mu^-]} \propto v^8 \left(\frac{m_c^2}{m_b^2}\right)^{2+|\lambda+\tilde{\lambda}|}, \quad (8)$$

where v denotes the characteristic velocity of the charm quark inside a charmonium.

Equation (8) implies that the helicity state which possesses the slowest asymptotic decrease is the one that conserves the hadron helicities $|\lambda + \tilde{\lambda}| = 0$. In line with the angular momentum conservation, the only possible configuration is $(\lambda, \tilde{\lambda}) = (0, 0)$. For each unit of the violation of the helicity conservation, there is a further suppression factor of $1/m_b^2$. In the limit $m_b \to \infty$, perhaps only the (0, 0) helicity state is phenomenologically relevant. Note that in NRQCD factorization language, the charm quark is also treated as heavy, and in fact its mass acts as the agent of violating the hadron helicity conservation.

We note that the power-law scaling specified in (8) is, in general, subject to the mild modifications due to the $\ln(m_b^2/m_c^2)$ from the loop contribution. This logarithmic scaling violation will be examined in detail in Sec. III.

III. THE CALCULATION OF THE HELICITY AMPLITUDES IN NRQCD FACTORIZATION APPROACH

The hard exclusive decay process $\Upsilon \to J/\psi + \chi_{cJ}$ ($J = 0, 1, 2$) is characterized by two hard scales set by the bottom and charm quark masses. This process can proceed via three separate channels: the $b\bar{b}$ pair first annihilates into a single photon, or three gluons, or two gluons plus a photon, subsequently the highly virtual photon/gluons transition into two $c\bar{c}$ pairs, which finally materialize into two fast-moving charmonium states.

Two influential perturbative QCD approaches are legitimate to describe such type of decay process, i.e., the light-cone approach [44,45] which is based on twist expansion, and the NRQCD factorization approach [33] that is based on the quark velocity expansion. As was seen in Sec. II, most helicity channels associated with the process $\Upsilon \to J/\psi + \chi_{c0,1,2}$ are of helicity-suppressed type. This feature impairs the practical usefulness of the light-cone approach, since the higher-twist light-cone distribution amplitudes of charmonia are rather poorly understood at present.

On the other hand, the NRQCD factorization approach, which is based upon a completely different expansion strategy, does not confront any obstacle in dealing with helicity-flipped channels. In the past two decades, this framework has been widely applied to numerous quarkonium decay and production processes [33]. In contrast with the light-cone approach, the nonperturbative input parameters in NRQCD factorization approach are numbers (local NRQCD matrix elements, or wave functions at the origin) rather than functions (light-cone distribution amplitudes). In this regard, NRQCD approach seems to be more economic and predictive than the light-cone approach.

In this work, we will investigate the process $\Upsilon \to J/\psi + \chi_{c0,1,2}$ in the framework of NRQCD factorization, incorporating aforementioned three distinct decay mechanisms.[3] We will be content with the lowest order accuracy in both the velocity expansion and the strong-coupling constant expansion. We are aware that our results may be subject to considerable uncertainty from various sources, yet still hope the predicted decay rates may capture the correct order of magnitude.

At the LO in the bottom and charm velocity, one can expedite the NRQCD approach calculation by invoking the covariant projection method [17], i.e., first calculate the on-shell T-matrix for $b\bar{b}(Q) \to c\bar{c}(P) + c\bar{c}(\tilde{P})$, then project each quark-antiquark pair onto the intended spin, color, and orbital angular momentum states. In this case, all the involved nonperturbative quarkonium-to-vacuum NRQCD matrix elements can be well approximated by three (the first derivative of) wave functions at the origin for the quarkonia Υ, J/ψ, and χ_{cJ}: $R_\Upsilon(0)$, $R_{J/\psi}(0)$, and $R'_{\chi_{cJ}}(0)$. Each of them can be either obtained from the quark potential models, or calculated from lattice simulation, or directly extracted from the quarkonia decay data.

The product of these three nonperturbative wave functions at the origin ubiquitously enters each helicity amplitude. Thus it seems convenient to define a reduced dimensionless helicity amplitude, of which these nonperturbative factors are explicitly pulled out. First, let us introduce a mass ratio variable,

$$r \equiv \frac{m_c^2}{m_b^2}. \tag{9}$$

The reduced helicity amplitude, dubbed $a^J_{\lambda,\tilde{\lambda}}$, is related to the standard helicity amplitude as follows:

$$\mathcal{A}^J_{\lambda,\tilde{\lambda}} \equiv -\sqrt{8\pi} N_c^{\frac{3}{2}} \frac{R_\Upsilon(0) R_{J/\psi}(0) R'_{\chi_c}(0)}{\sqrt{m_b} m_c^4} r^{1+\frac{1}{2}|\lambda+\tilde{\lambda}|} a^J_{\lambda,\tilde{\lambda}}, \tag{10}$$

where $N_c = 3$ denotes the number of colors. Note that the scaling factor dictated by the HSR has been explicitly factored out, the reduced amplitude $a^J_{\lambda,\tilde{\lambda}}$ is thereby expected to scale with r as $\mathcal{O}(r^0)$.

Inserting (10) back into (5), one can reexpress the integrated polarized decay rate as

$$\begin{aligned}\Gamma[\Upsilon \to J/\psi(\lambda) + \chi_{cJ}(\tilde{\lambda})] &= N_c^3 R_\Upsilon^2(0) R_{J/\psi}^2(0) R'^2_{\chi_{cJ}}(0) \frac{|\mathbf{P}|}{3M_\Upsilon^2 m_b m_c^8} r^{2+|\lambda+\tilde{\lambda}|} \\ &\times \left| a^J_{\gamma;\lambda,\tilde{\lambda}} + a^J_{3g;\lambda,\tilde{\lambda}} + a^J_{\gamma gg;\lambda,\tilde{\lambda}} \right|^2 \end{aligned} \tag{11}$$

for each helicity channel. The subscripts γ, $3g$, and γgg emphasize the decay channel with which the reduce amplitude is affiliated. Obviously, it is of interest to ascertain the relative strength and phase among these different types of amplitudes.

In the remainder of this section, we will present the analytic expressions of the reduced helicity amplitudes associated with each decay channel.

A. Single-photon channel

We start by considering the decay channel $\Upsilon \to \gamma^* \to J/\psi + \chi_{cJ}$, with some typical LO diagrams shown in Fig. 1. This process is very similar to the continuum $J/\psi + \chi_{cJ}$ production in e^+e^- annihilation [17].

After obtaining the decay amplitude $\mathcal{A}^J_\gamma$ in NRQCD factorization, one can employ the helicity projectors enumerated in the Appendix to project out 10 corresponding helicity amplitudes. It is straightforward to follow Eq. (10) to read off the reduced helicity amplitude in the single-photon channel,

$$a^J_{\gamma;\lambda,\tilde{\lambda}} = \frac{N_c^2 - 1}{N_c^2} e_b e_c \alpha \alpha_s c^J_{\lambda,\tilde{\lambda}}(r), \tag{12}$$

where $e_b = -\frac{1}{3}$ and $e_c = \frac{2}{3}$ are the electric charges of the b and c quarks, α and α_s are the QED and QCD coupling constants, respectively. The coefficient functions $c^J_{\lambda,\tilde{\lambda}}(r)$ read

$$c^0_{0,0}(r) = 1 + 10r - 12r^2 + 2ry \qquad c^0_{1,0}(r) = 9 - 14r - \frac{y}{2}\left(\frac{1}{r} - 6\right), \tag{13a}$$

$$c^1_{0,1}(r) = -\sqrt{6}\left[2 - 7r + \frac{3}{2}y\right] \qquad c^1_{1,0}(r) = -\sqrt{6}\left[r + \frac{y}{2}\left(\frac{1}{r} - 1\right)\right] \qquad c^1_{1,1}(r) = -2\sqrt{6}\left[1 - 3r + \frac{y}{4}\left(\frac{1}{r} + 2\right)\right], \tag{13b}$$

$$c^2_{0,0}(r) = \sqrt{2}[1 - 2r - 12r^2 + 2ry] \qquad c^2_{0,1}(r) = \sqrt{6}\left[1 - 5r + \frac{y}{2}\right] \qquad c^2_{1,0}(r) = \sqrt{2}\left[3 - 11r - \frac{y}{2}\left(\frac{1}{r} - 3\right)\right]$$

$$c^2_{1,1}(r) = 2\sqrt{6}\left[1 - 3r - \frac{y}{4}\left(\frac{1}{r} - 2\right)\right] \qquad c^2_{1,2}(r) = \sqrt{3}\left[2 - \frac{y}{r}\right], \tag{13c}$$

where $y \equiv -\alpha/\alpha_s$. The y-dependent terms characterize the photon fragmentation contributions, as depicted in Fig. 1(b), which are often accompanied by an enhancement factor $1/r$ for the transversely polarized J/ψ.

[3]Unlike the exclusive double-charmonium production in e^+e^- annihilation, where a factorization theorem in NRQCD has been proved to all orders in α_s [46], there has not yet existed any rigorous proof for the validity of NRQCD approach to $\Upsilon \to J/\psi + \chi_{c0,1,2}$.

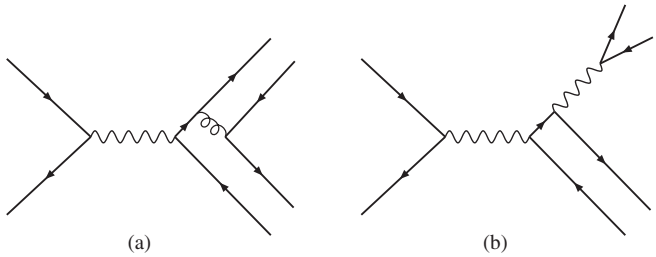

FIG. 1. Two representative lowest-order diagrams that contribute to $\Upsilon \to \gamma^* \to J/\psi + \chi_{cJ}$. There are in total four diagrams in class (a) and two in class (b).

Barring the pure QED fragmentation contributions, these 10 coefficient functions agree, up to an immaterial phase, with those associated with the process $e^+e^- \to J/\psi + \chi_{c0,1,2}$ [32]. It is interesting to mention that, for some accidental reason, the QCD part of the single-photon $J/\psi(\pm 1) + \chi_{c1}(0)$ amplitude receives an extra suppression factor than implied from HSR.

B. Three-gluon channel

Next we turn to the strong decay channel $\Upsilon \to 3g \to J/\psi + \chi_{cJ}$, which supposedly makes the most significant contribution. Some of the representative LO diagrams have been illustrated in Fig. 2. In contrast with the single-photon channel, this channel first starts at the one-loop level. The charge conjugation invariance guarantees that one needs only retain those diagrams with "Abelian" gluon topology as shown in Fig. 2.

After obtaining the decay amplitude $\mathcal{A}^J_{3g}$ using the covariant projection technique, and prior to performing the loop integration, we apply those helicity projection operators given in the Appendix to project out 10 corresponding helicity amplitudes. This operation brings forth great simplification, because all the polarization vectors (tensors) of Υ, J/ψ, and χ_{cJ} have been eliminated from the integrand, and the numerators in loop integrals now become Lorentz scalars comprised entirely of the external and loop momenta.

It is then straightforward to utilize the partial fractioning technique to reduce all the higher-point one-loop integrals into a set of 2-point and 3-point scalar integrals. Most of the encountered scalar integrals can be found in the Appendix of Ref. [13], whose accuracy has been numerically checked by the MATHEMATICA package LOOPTOOLS [47]. There also arise some nonstandard 2- and 3-point scalar integrals, which contain propagators with quadratic power due to the projection of the P-wave state. All of their analytic expressions can be readily worked out.

As a cross-check, we also employ the MATHEMATICA package FIRE [48] and the code APART [49] to perform an independent calculation. Thanks to the integration-by-part algorithm built in FIRE, it turns out that all the required master integrals (MIs) become just the conventional 2-point and 3-point scalar integrals as given in Ref. [13]. The final results generated by this more automatic approach exactly coincides with those obtained from the partial-fractioning method.

As a third consistency check, the calculation is redone by exchanging the order between helicity projection and loop integration. That is, we first utilize the programs APART and FIRE at the amplitude level, which are more cumbersome and time-consuming, yet still technically feasible. Once the IR-finite T-matrices are obtained, we then project out each intended helicity amplitudes at the very end. We again find the exact agreement with the previous two methods. This calculation can be viewed as a strong support for the validity of the four-dimensional helicity projectors given in the Appendix.

Each individual diagram in Fig. 2, being ultraviolet convergent, albeit contains logarithmic infrared divergence. Dimensional regularization is adopted to regularize those IR singularities. Upon summing all the diagrams, the ultimate expression for each helicity amplitude becomes IR finite, which endorses the validity of NRQCD factorization approach for these exclusive Υ decay processes.

Following (10), we express the reduced helicity amplitude in the three-gluon channel as

$$a^J_{3g;\lambda,\tilde{\lambda}} = \frac{(N_c^2-1)(N_c^2-4)}{N_c^4}\,\frac{\alpha_s^3}{8\pi}\,\frac{m_b^2}{m_b^2-4m_c^2}\,f^J_{\lambda,\tilde{\lambda}}(r). \qquad (14)$$

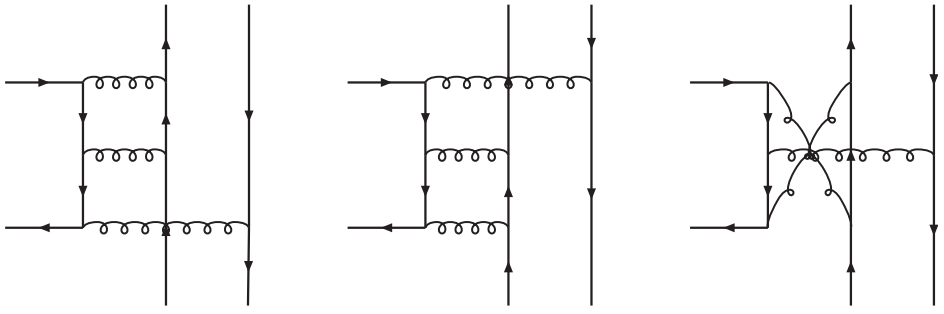

FIG. 2. Some representative lowest-order diagrams that contribute to $\Upsilon \to 3g \to J/\psi + \chi_{cJ}$.

The color factor reflects the fact that the three "Abelian" gluons in Fig. 2 must bear an odd C-parity, thus proportional to $d^{abc}d^{abc} = (N_c^2 - 1)(N_c^2 - 4)/N_c$, where d^{abc} denotes the totally symmetric structure constants of $SU(N_c)$ group.

All the loop effects are encapsulated in the complex-valued dimensionless functions $f^J_{\lambda,\tilde{\lambda}}(r)$. Their full expressions are somewhat lengthy, so will not be reproduced here.[4] On the other hand, the profiles of these functions over a wide range of r are explicitly shown in Figs. 3–5.

Theoretically, it is interesting to ascertain the asymptotic behaviors of these reduced helicity amplitudes in the limit $m_b \gg m_c$. As mentioned before, we anticipate to see the logarithm scaling violation to the naive power-law scaling given in (8). The asymptotic expressions of the $f^J_{\lambda,\tilde{\lambda}}$ functions read ($J = 0, 1, 2$)

$$f^0_{0,0}(r) = -4 + \frac{2\pi}{3\sqrt{3}} + \frac{2\pi^2}{9} + \frac{2\pi i}{3} + \mathcal{O}(r\ln^2 r), \tag{15a}$$

$$f^0_{1,0}(r) = -\ln^2 r - 7\ln r - \frac{\pi^2}{9} + \frac{25\pi}{\sqrt{3}} - \frac{73}{6} - 2\pi i(\ln r + 3) + \mathcal{O}(r\ln^2 r), \tag{15b}$$

$$f^1_{0,1}(r) = \sqrt{6}\left(\frac{2}{3}\ln r + \frac{\pi^2}{3} - \frac{17\pi}{2\sqrt{3}} + \frac{73}{9} + 3\pi i\right) + \mathcal{O}(r\ln r), \tag{15c}$$

$$f^1_{1,0}(r) = \sqrt{6}\left[-\ln^2 r - 3\ln r + \frac{\pi^2}{9} - \frac{8\pi}{\sqrt{3}} + \frac{23}{6} - 2\pi i\left(\ln r + \frac{1}{3}\right)\right] + \mathcal{O}(r\ln^2 r), \tag{15d}$$

$$f^1_{1,1}(r) = \sqrt{6}\left[-\ln^2 r - \frac{7}{2}\ln r - \frac{8\pi^2}{9} - \frac{7\pi}{3\sqrt{3}} - \frac{25}{12} - 2\pi i\left(\ln r - \frac{7}{6}\right)\right] + \mathcal{O}(r\ln^2 r), \tag{15e}$$

$$f^2_{0,0}(r) = \sqrt{2}\left(\frac{2\pi^2}{9} + \frac{2\pi}{3\sqrt{3}} - 4 + \frac{2\pi i}{3}\right) + \mathcal{O}(r\ln^2 r), \tag{15f}$$

$$f^2_{0,1}(r) = \sqrt{6}\left(-\frac{2}{3}\ln r + \frac{5\pi^2}{9} - \frac{7\pi}{2\sqrt{3}} - \frac{13}{9} - \frac{\pi i}{3}\right) + \mathcal{O}(r\ln^2 r), \tag{15g}$$

$$f^2_{1,0}(r) = \sqrt{2}\left[-\ln^2 r - 7\ln r + \frac{11\pi^2}{9} - \frac{11\pi}{\sqrt{3}} + \frac{23}{6} - 2\pi i(\ln r + 1)\right] + \mathcal{O}(r\ln^2 r), \tag{15h}$$

$$f^2_{1,1}(r) = \sqrt{6}\left[-\ln^2 r - \frac{15}{2}\ln r - \frac{8\pi^2}{9} + \frac{25\pi}{3\sqrt{3}} - \frac{145}{12} - 2\pi i\left(\ln r + \frac{3}{2}\right)\right] + \mathcal{O}(r\ln^2 r), \tag{15i}$$

$$f^2_{1,2}(r) = \sqrt{3}\left[-2\ln^2 r - 10\ln r + \frac{10\pi^2}{9} - \frac{20\pi}{\sqrt{3}} + \frac{89}{3} - 4\pi i\left(\ln r + \frac{1}{3}\right)\right] + \mathcal{O}(r\ln^2 r). \tag{15j}$$

For the reader's convenience, all the asymptotic results of $f^J_{\lambda,\tilde{\lambda}}(r)$ are also shown in Figs. 3–5 juxtaposed with the corresponding exact results. We observe that for most helicity configurations, the asymptotic results do not coincide well with the exact ones at the phenomenologically relevant point $r = m_c^2/m_b^2 \approx 0.10$.

From (15), one confirms that the scaling violation is indeed of the logarithmic form. More interestingly, we see that the occurrence of the double-logarithm $\ln^2 r$ is always affiliated with the helicity-suppressed ($|\lambda + \tilde{\lambda}| > 0$) decay channels. This is similar to the empirical patterns observed for double charmonium production in e^+e^- annihilation in Refs. [32,50]. Moreover, such double logarithms have previously also been observed in the helicity-suppressed bottomonium exclusive decay processes, e.g., $\Upsilon \to J/\psi + \eta_c$ [13], $\eta_b \to J/\psi J/\psi$ [4]. The light-cone approach is presumably the proper tool to handle these process-dependent double logarithms, since it provides a natural means to disentangle the contributions from the two disparate scales m_b and m_c. Unfortunately, this approach is known to have some notorious difficulty in dealing with the helicity-suppressed hard exclusive reactions such as the $\gamma^*\rho\pi$ form factor [45], because the

[4]In our previous calculation as reported in Ref. [34], prior to performing the loop integration, we erroneously carried out the Dirac trace in four spacetime dimensions. This is an unfortunate mistake, which contradicts the spirit of Dimensional regularization. In the current work, we take all the Lorentz vectors (both loop and external momenta) as the $D = 4 - 2\epsilon$ dimensional objects when calculating the Dirac trace. However, we would like to stress that the helicity projectors listed in the Appendix, which are derived by simply assuming $D = 4$, are still applicable in this situation. That is because the ultimate amplitudes are UV, IR finite, so it does not matter whether the external momenta are taken as $4 - 2\epsilon$- or four-dimensional in the intermediate steps. Finally, we note that the analytic expressions of the various reduced helicity amplitudes in the three-gluon channel for $\Upsilon \to J/\psi + \chi_{c0,1,2}$ markedly differ from those given in Ref. [34].

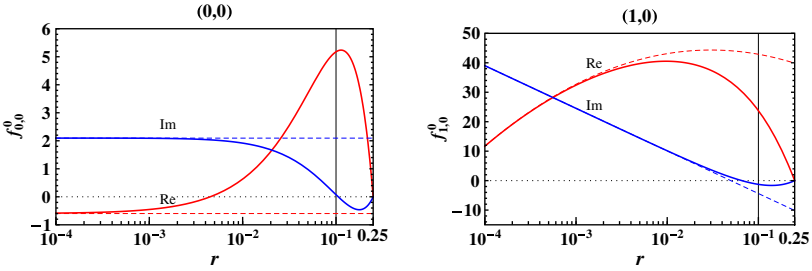

FIG. 3 (color online). Real and imaginary parts of $f^0_{\lambda,\tilde{\lambda}}(r)$. The solid curves correspond to the exact results, and the dashed curves represent the asymptotic ones taken from (15a) and (15b). The vertical mark is placed at the phenomenologically relevant point $r = 0.10$.

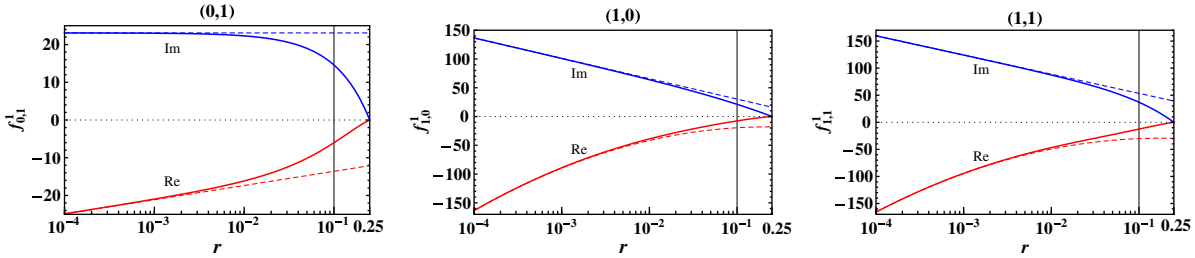

FIG. 4 (color online). Real and imaginary parts of $f^1_{\lambda,\tilde{\lambda}}(r)$. The solid curves correspond to the exact results, and the dashed curves represent the asymptotic ones taken from (15c) to (15e).

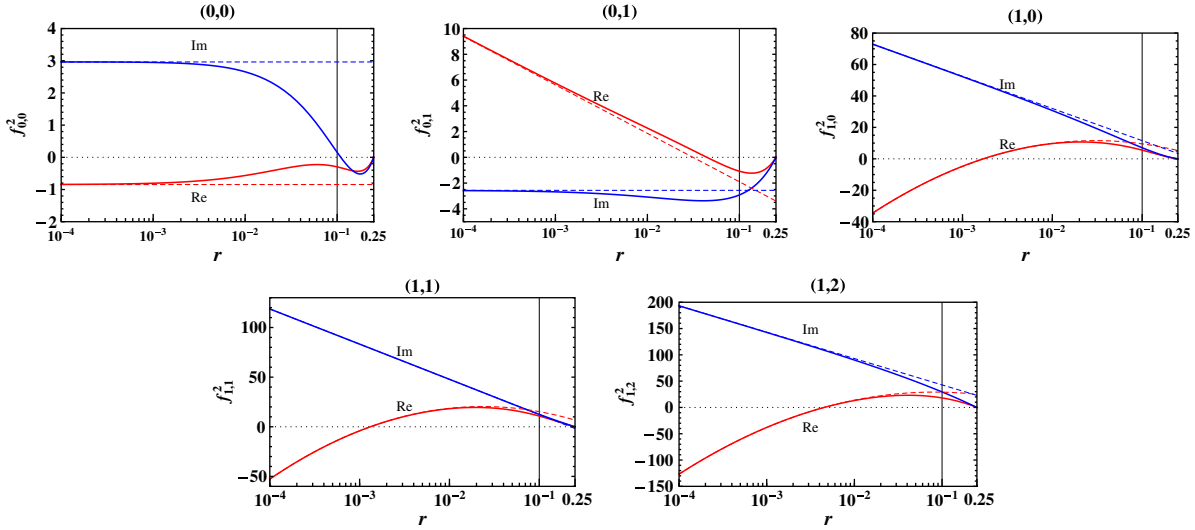

FIG. 5 (color online). Real and imaginary parts of $f^2_{\lambda,\tilde{\lambda}}(r)$. The solid curves correspond to the exact results, and the dashed curves represent the asymptotic ones taken from (15f) to (15j).

endpoint singularity in the convolution integral encountered in such processes hindered one's capability of performing the consistent higher order calculation. Consequently, at present one seems unable to have a systematic control over these double logarithms appearing in the one-loop NRQCD short-distance coefficients in the exclusive double charmonium production from e^+e^- annihilation [50]. For the exclusive double charmonium production processes from Υ decay, the double logarithms of form $\ln^2 m_b^2/m_c^2$ already arise at the lowest order in α_s of the strong decay channel (though appear at the one-loop level). The origin of these double logarithms is likely quite different from that associated with the double charmonium production from e^+e^- annihilation. It may be instructive to

carry out a light-cone calculation for the processes studied in this work, to see whether one can reproduce these large double logarithms or not.

Finally we mention one peculiarity associated with the helicity channel $\Upsilon \to J/\psi(\lambda = \pm 1) + \chi_{c1}(\tilde{\lambda} = 0)$. Recall that at LO in α_s, this helicity amplitude from the single-photon channel is suppressed by an extra factor of r with respect to the HSR, as can be seen in (13b). Nevertheless, from (15d) we find that this helicity amplitude in the $3g$ channel just possesses the correct power-law scaling as dictated by the HSR. This implies that the power suppression of the LO single-photon amplitude is purely accidental.

C. One-photon–two-gluon channel

From the ratios of the measured inclusive Υ decay rates in three different channels, as listed in (2), an educated guess is that the exclusive decay channel $\Upsilon \to \gamma gg \to J/\psi + \chi_{cJ}$ yields the least important contribution. Nevertheless, for the sake of completeness, let us finally assess the contribution from this radiative decay channel.

Similar to the strong decay channel, this radiative decay channel also starts at the one-loop order. Some typical LO diagrams have been illustrated in Fig. 6. For simplicity, and to be commensurate with the approximation adopted for the single-photon channel in Sec. III A, we only retain those photon-fragmentation diagrams, whereas the neglected diagrams are identical to those in Fig. 2 except with the gluon outside the loop replaced by the photon. We wish that these fragmentation-type diagrams constitute the dominant contributions, which is certainly the case for the transversely polarized J/ψ.

Following the steps outlined in Sec. III B, one then projects out the 10 required helicity amplitudes, with all the polarization vectors (tensors) of Υ, J/ψ and χ_{cJ} eliminated from the loop integral. Nevertheless, it appears to be less straightforward than in the three-gluon channel to employ the partial fraction to simplify the encountered one-loop integrals.

Fortunately, the powerful MATHEMATICA packages FIRE [48] and APART [49] can still be successfully applied to reduce the general higher-point tensor one-loop integrals into a set of MIs. With the aid of the integration-by-part algorithm built in FIRE, all the involved MIs become just the standard 2-point and 3-point scalar integrals. The analytic expressions of these scalar integrals can be found in Refs. [13,51], whose correctness have been numerically verified by using LOOPTOOLS [47].

Analogous to the three-gluon decay channel, each individual diagram in Fig. 6 is UV finite but IR divergent. After summing all the diagrams, the ultimate expression for each helicity amplitude turns out to be completely IR finite.

In accordance with (10), the reduced helicity amplitude in the radiative decay channel can be expressed as

$$a^J_{\gamma gg;\lambda,\tilde{\lambda}} = \frac{N_c^2 - 1}{N_c^2} \frac{e_b e_c \alpha \alpha_s^2}{4\pi} \frac{m_b^2}{m_b^2 - 4m_c^2} r^{-|\lambda|} g^J_{\lambda,\tilde{\lambda}}(r). \quad (16)$$

The inclusion of an extra factor $r^{-|\lambda|}$ is reminiscent of the photon fragmentation mechanism: when the J/ψ becomes transversely polarized ($\lambda = \pm 1$), the corresponding helicity amplitude would receive a $1/r$ enhancement with respect to the nominal HSR.

All the loop effects are encoded in the complex-valued, dimensionless functions $g^J_{\lambda,\tilde{\lambda}}(r)$. Their full expressions are somewhat lengthy and will not be reproduced here. On the other hand, the profiles of these functions over a wide range of r are shown in Figs. 7–9.

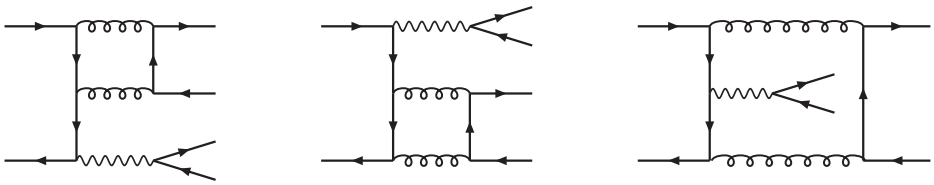

FIG. 6. Some representative lowest-order diagrams that contribute to $\Upsilon \to \gamma gg \to J/\psi + \chi_{cJ}$.

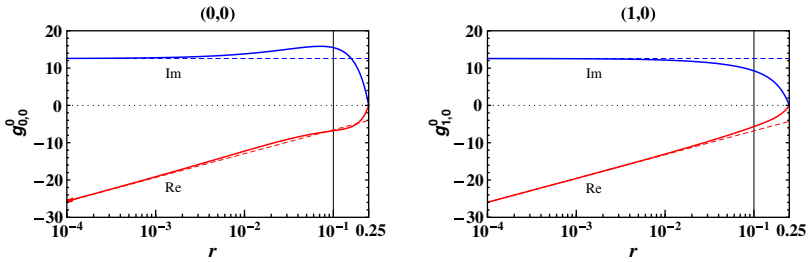

FIG. 7 (color online). Real and imaginary parts of $g^0_{\lambda,\tilde{\lambda}}(r)$. The solid curves correspond to the exact results, and the dashed curves represent the asymptotic ones taken from (17a) and (17b). The vertical mark is placed at the phenomenologically relevant point $r = 0.10$.

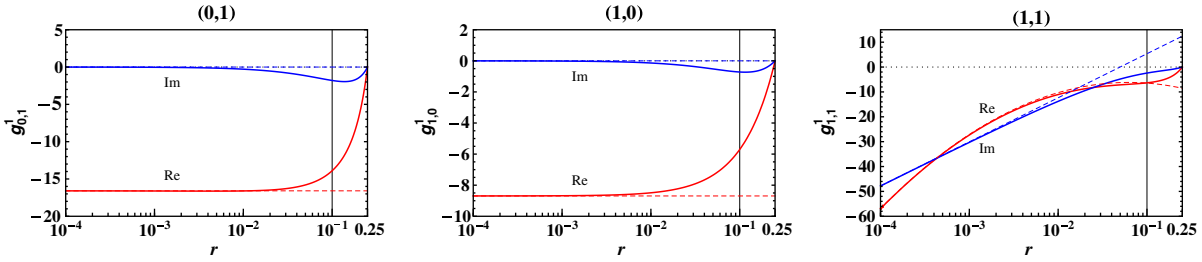

FIG. 8 (color online). Real and imaginary parts of $g^1_{\lambda,\tilde{\lambda}}(r)$. The solid curves correspond to the exact results, and the dashed curves represent the asymptotic ones taken from (17c) to (17e).

We are curious to know the asymptotic behavior of the reduced helicity amplitudes in this decay channel. After some manipulations, we find the asymptotic expressions of the functions $g^J_{\lambda,\tilde{\lambda}}$ $(J = 0, 1, 2)$ to read

$$g^0_{0,0}(r) = 4\ln 2\ln r - \frac{\pi^2}{3} - 4\ln 2 + \frac{53}{9} + 4\pi i + \mathcal{O}(r\ln^2 r), \tag{17a}$$

$$g^0_{1,0}(r) = 4\ln 2\ln r + \frac{5\pi^2}{12} - 8\ln 2 + 1 + 4\pi i + \mathcal{O}(r\ln^2 r), \tag{17b}$$

$$g^1_{0,1}(r) = -4\sqrt{6}(\ln 2 + 1) + \mathcal{O}(r\ln r), \tag{17c}$$

$$g^1_{1,0}(r) = \sqrt{6}\left(2\ln 2 - \frac{\pi^2}{2}\right) + \mathcal{O}(r\ln r), \tag{17d}$$

$$g^1_{1,1}(r) = -\sqrt{6}\left[\frac{1}{2}\ln^2 r + 4\ln 2\ln r + \frac{\pi^2}{12} + 8\ln 2 - \pi i(\ln r + 3)\right] + \mathcal{O}(r\ln^2 r), \tag{17e}$$

$$g^2_{0,0}(r) = \sqrt{2}\left(4\ln 2\ln r - \frac{\pi^2}{3} + 12\ln 2 - \frac{17}{9} - 4\pi i\right) + \mathcal{O}(r\ln^2 r), \tag{17f}$$

$$g^2_{0,1}(r) = \sqrt{6}(2 - 4\ln 2) + \mathcal{O}(r\ln r), \tag{17g}$$

$$g^2_{1,0}(r) = \sqrt{2}\left(4\ln 2\ln r + \frac{5\pi^2}{12} + 8\ln 2 - 3 - 4\pi i\right) + \mathcal{O}(r\ln r), \tag{17h}$$

$$g^2_{1,1}(r) = \sqrt{6}\left[-\frac{1}{2}\ln^2 r - 4\ln 2\ln r + 4\ln r + \frac{5\pi^2}{12} - \frac{20}{3}\ln 2 + \frac{23}{3} + \pi i\left(\ln r - \frac{5}{3}\right)\right] + \mathcal{O}(r\ln^2 r), \tag{17i}$$

$$g^2_{1,2}(r) = \sqrt{3}\left[-2\ln^2 r - 4\ln r + \frac{5\pi^2}{6} + \frac{16}{3}\ln 2 - \frac{16}{3} + 2\pi i\left(2\ln r + \frac{5}{3}\right)\right] + \mathcal{O}(r\ln r). \tag{17j}$$

In Figs. 7–9 we also juxtapose these asymptotic results of $g^J_{\lambda,\tilde{\lambda}}(r)$ with the exact results. For most helicity configurations, the asymptotic results seem not to converge well with the exact ones for the phenomenologically relevant point $r = m_c^2/m_b^2 \approx 0.10$.

A quick survey on (17) reveals that that the scaling violation is again of the logarithmic form. More interestingly, the same pattern of double logarithms still holds: the occurrence of the double-logarithm $\ln^2 r$ is always affiliated with the helicity-suppressed decay channels.

We close this section by making a simple observation. As can be seen from Fig. 8, the imaginary parts of the functions $g^1_{\lambda,\tilde{\lambda}}$ are generally nonzero, though some of these vanish asymptotically. At first sight, this may contradict Landau-Yang theorem because $\chi_{c1} \to gg$ should be strictly forbidden. This implies that though the apparent two-gluon cuts in Fig. 6 do not contribute, the other cuts that simultaneously pass through the bottom and charm quark lines must yield nonvanishing contributions to the imaginary parts for $\Upsilon \to J/\psi + \chi_{c1}$.

IV. PHENOMENOLOGY

We are now in a position to make concrete predictions for the decay rates of $\Upsilon \to J/\psi + \chi_{c0,1,2}$, by plugging (12), (14), and (16) into (11).

In the numerical analysis, we take the following various bottomonia and charmonia masses from the 2012 Particle Data Group compilation [1]: $M_{\Upsilon(1S)} = 9.460$ GeV, $M_{\Upsilon(2S)} = 10.023$ GeV, $M_{\Upsilon(3S)} = 10.355$ GeV, $M_{J/\psi} = 3.097$ GeV, $M_{\chi_{c0}} = 3.415$ GeV, $M_{\chi_{c1}} = 3.511$ GeV, $M_{\chi_{c2}} = 3.556$ GeV. These inputs are used to determine $|\mathbf{P}|$ according to (4), which appears in the phase space

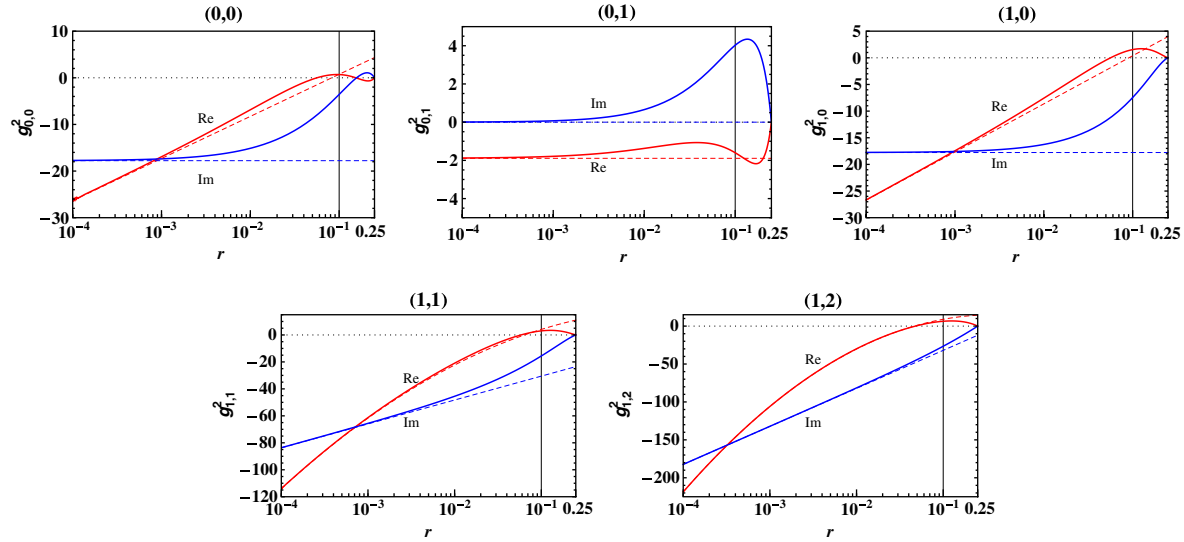

FIG. 9 (color online). Real and imaginary parts of $g^2_{\lambda,\tilde{\lambda}}(r)$. The solid curves correspond to the exact results, and the dashed curves represent the asymptotic ones taken from (17f) to (17j).

factor in (11). To calculate the squared matrix elements, particularly the functions $f^J_{\lambda,\tilde{\lambda}}(r)$ and $g^J_{\lambda,\tilde{\lambda}}(r)$, we instead adopt the following values for the quark masses: $m_c = 1.5$ GeV, $m_b = 4.7$ GeV, corresponding to $r = 0.102$. Later we also wish to predict the branching fractions for the decays $\Upsilon(nS) \to J/\psi + \chi_{c0,1,2}$ ($n = 1, 2, 3$). For this purpose, we take the following total decay width of various Υ states from [1]: $\Gamma[\Upsilon(1S)] = 54.02$ keV, $\Gamma[\Upsilon(2S)] = 31.98$ keV, and $\Gamma[\Upsilon(3S)] = 20.32$ keV, respectively.

For simplicity, we fix the electromagnetic fine structure constant as $\alpha = 1/137$. For the strong coupling constant, any value evaluated with the renormalization scale ranging from $2m_b$ to $2m_c$ seems to be acceptable. This scale ambiguity constitutes one of the most important sources of theoretical uncertainty. Without much prejudice, we simply choose a medium value $\alpha_s(m_b) = 0.22$.

As for the wave functions at the origin for various quarkonia, we use the following values obtained from the Buchmüller-Tye potential model [52]: $|R_{\Upsilon(1S)}(0)|^2 = 6.477$ GeV^3, $|R_{\Upsilon(2S)}(0)|^2 = 3.234$ GeV^3, $|R_{\Upsilon(3S)}(0)|^2 = 2.474$ GeV^3, $|R_{J/\Psi}(0)|^2 = 0.81$ GeV^3, $|R'_{\chi_{c0,1,2}}(0)|^2 = 0.075$ GeV^5.

In Table I, we tabulate the values of the reduced helicity amplitudes a_γ, a_{3g}, and $a_{\gamma gg}$ associated with each helicity channel for $\Upsilon(1S) \to J/\psi + \chi_{c0,1,2}$. One sees that the relative phases among each amplitude vary channel by channel, and particularly there seems no universal phase pattern between the single-photon and three-gluon channel. Our finding contradicts the universal relative phase conjecture made in Ref. [53].

One curious question is whether the relative strength between three distinct decay mechanisms bears roughly the same pattern as that in Υ inclusive decay, as given in (2). A very crude guess is that each helicity amplitude for this exclusive decay process might be proportional to $\sqrt{\mathcal{B}_{\rm incl}}$, so that one naively expects

$$|a_\gamma|:|a_{3g}|:|a_{\gamma gg}| \approx 1{:}3.3{:}0.5 \tag{18}$$

for each helicity configuration.

TABLE I. The values of the reduced helicity amplitudes a_γ, a_{3g}, and $a_{\gamma gg}$ associated with each helicity channel for $\Upsilon(1S) \to J/\psi + \chi_{c0,1,2}$. For simplicity, a factor of 10^{-4} has been pulled out of each entry.

		(0, 0)	(1, 0)	(0, 1)	(1, 1)	(1, 2)
$J/\psi + \chi_{c0}$	a_γ	-5.99	-24.23	⋯	⋯	⋯
	a_{3g}	$18.33e^{i0.54^\circ}$	$82.87e^{-i3.19^\circ}$	⋯	⋯	⋯
	$a_{\gamma gg}$	$1.58e^{-i66.32^\circ}$	$1.01e^{-i58.59^\circ}$	⋯	⋯	⋯
$J/\psi + \chi_{c1}$	a_γ	⋯	-0.35	9.61	9.27	⋯
	a_{3g}	⋯	$78.04e^{i109.57^\circ}$	$54.94e^{i112.26^\circ}$	$135.67e^{i108.61^\circ}$	⋯
	$a_{\gamma gg}$	⋯	$5.23e^{i7.29^\circ}$	$1.30e^{i7.48^\circ}$	$6.20e^{i20.52^\circ}$	⋯
$J/\psi + \chi_{c2}$	a_γ	-2.98	-8.94	-3.68	-11.80	-12.78
	a_{3g}	$1.15e^{i157.72^\circ}$	$30.89e^{i51.71^\circ}$	$10.94e^{-i110.67^\circ}$	$57.18e^{i49.00^\circ}$	$120.16e^{i58.27^\circ}$
	$a_{\gamma gg}$	$0.33e^{i101.36^\circ}$	$6.89e^{i102.07^\circ}$	$0.41e^{-i68.19^\circ}$	$14.35e^{i101.39^\circ}$	$24.70e^{i103.90^\circ}$

TABLE II. The polarized and the polarization-summed partial widths and the corresponding branching fractions. $\Gamma_{\gamma}^{[J]}$, $\Gamma_{3g}^{[J]}$, and $\Gamma_{\gamma gg}^{[J]}$ represent the individual decay rates from the single-photon, three-gluon, and one-photon–two-gluon channels affiliated with the process $\Upsilon(1S) \to J/\psi + \chi_{cJ}$ ($J = 0, 1, 2$), respectively, while $\Gamma_{\rm tot}^{[J]}$ denotes the decay rate which incorporates all three decay mechanisms according to (11). The two rightmost columns also give the unpolarized decay rates and branching fractions by summing over all possible helicity configurations. All the partial decay widths are in units of eV.

	(0, 0)	(1, 0)	(0, 1)	(1, 1)	(1, 2)	Unpol	$\mathcal{B}$
$\Gamma_{\gamma}^{[0]}$	4.2×10^{-3}	7.0×10^{-3}	$\cdots$	$\cdots$	$\cdots$	1.8×10^{-2}	3.3×10^{-7}
$\Gamma_{3g}^{[0]}$	3.9×10^{-2}	8.2×10^{-2}	$\cdots$	$\cdots$	$\cdots$	2.0×10^{-1}	3.7×10^{-6}
$\Gamma_{\gamma gg}^{[0]}$	2.9×10^{-4}	1.2×10^{-3}	$\cdots$	$\cdots$	$\cdots$	2.6×10^{-3}	4.8×10^{-8}
$\Gamma_{\rm tot}^{[0]}$	1.4×10^{-2}	2.8×10^{-2}	$\cdots$	$\cdots$	$\cdots$	7.0×10^{-2}	1.3×10^{-6}
$\Gamma_{\gamma}^{[1]}$	$\cdots$	1.4×10^{-6}	1.1×10^{-3}	1.0×10^{-4}	$\cdots$	2.4×10^{-3}	4.4×10^{-8}
$\Gamma_{3g}^{[1]}$	$\cdots$	7.1×10^{-2}	3.5×10^{-2}	2.2×10^{-2}	$\cdots$	2.6×10^{-1}	4.8×10^{-6}
$\Gamma_{\gamma gg}^{[1]}$	$\cdots$	3.2×10^{-4}	2.0×10^{-5}	4.6×10^{-5}	$\cdots$	7.7×10^{-4}	1.4×10^{-8}
$\Gamma_{\rm tot}^{[1]}$	$\cdots$	6.2×10^{-2}	4.7×10^{-2}	2.3×10^{-2}	$\cdots$	2.6×10^{-1}	4.9×10^{-6}
$\Gamma_{\gamma}^{[2]}$	1.0×10^{-3}	9.3×10^{-4}	1.6×10^{-4}	1.7×10^{-4}	2.0×10^{-5}	3.6×10^{-3}	6.7×10^{-8}
$\Gamma_{3g}^{[2]}$	1.5×10^{-4}	1.1×10^{-2}	1.4×10^{-3}	3.9×10^{-3}	1.7×10^{-3}	3.6×10^{-2}	6.7×10^{-7}
$\Gamma_{\gamma gg}^{[2]}$	1.2×10^{-5}	5.5×10^{-4}	2.0×10^{-6}	2.4×10^{-4}	7.4×10^{-5}	1.8×10^{-3}	3.3×10^{-8}
$\Gamma_{\rm tot}^{[2]}$	5.3×10^{-4}	2.6×10^{-3}	5.5×10^{-4}	1.1×10^{-3}	8.3×10^{-4}	1.1×10^{-2}	2.0×10^{-7}

Inspecting Table I, we find that for many helicity configurations, the three distinct helicity amplitudes do exhibit a similar hierarchy as that given in (18), i.e., $|a_{3g}| > |a_{\gamma}| > |a_{\gamma gg}|$, though the radiative decay amplitude are often much more suppressed. However, there are also a few notable exceptions, e.g., for the polarized decays $\Upsilon \to J/\psi(\pm 1) + \chi_{c1}(0)$,[5] $\Upsilon \to J/\psi(\pm 1) + \chi_{c2}(\pm 1)$, $\Upsilon \to J/\psi(\pm 1) + \chi_{c2}(\pm 2)$, the magnitude of the radiative decay amplitudes is comparable, or even greater, than that of the single-photon amplitudes; for the decay $\Upsilon \to J/\psi(0) + \chi_{c2}(0)$, the single-photon amplitude is even greater in magnitude than the respective three-gluon amplitude.

In Table II, we also list the polarized decay widths for $\Upsilon(1S) \to J/\psi(\lambda) + \chi_{c0,1,2}(\tilde{\lambda})$ for each independent helicity configurations $(\lambda, \tilde{\lambda})$, together with the polarization-summed results. To readily visualize the interference effect among three distinct decay mechanisms, we also tabulate the individual decay rates from the single-photon, three-gluon, and one-photon-two-gluon channels, respectively, as well as the full decay rate given by (11). Table II reveals that a_{γ} and a_{3g} in $\Upsilon(1S) \to J/\psi + \chi_{c0,2}$ are subject to destructive interference.

The hierarchy among the polarized decay widths in different helicity configurations, from either an individual decay mechanism or the complete contributions, seems hardly to obey the HSR as indicated in (8). The pattern is abnormal for $\Upsilon \to J/\psi + \chi_{c0}$, where the helicity-suppressed $(\pm 1, 0)$ channel even possesses a bigger decay rate than the helicity-favored (0, 0) channel; for $\Upsilon \to J/\psi + \chi_{c2}$, the largest polarized decay rates are associated with the helicity-suppressed configurations $(\pm 1, 0)$ and $(\pm 1, \pm 1)$, whereas the smallest polarized decay rate is associated with the HSR-favored (0, 0) state.[6] These symptoms can presumably be attributed to the fact that the mass ratio $m_c/m_b \approx 1/3$ might not be small enough to warrant the asymptotic counting rule.

Finally in Table III, we tabulate our predictions of the partial decay widths, which are calculated according to (7), together with the corresponding branching fractions, for the various processes $\Upsilon(nS) \to J/\psi + \chi_{c0,1,2}$ ($n = 1, 2, 3$). All the three decay mechanisms are incorporated. We observe that the decay branching fractions satisfy the ordering[7] $\mathcal{B}^{[1]} > \mathcal{B}^{[0]} \gg \mathcal{B}^{[2]}$, with the first two reaching the order of 10^{-6}. We note that all these predicted branching ratios are compatible with the various experimental bounds on J/ψ or χ_{cJ} inclusive production rates in $\Upsilon(1S, 2S)$ decays, as given in (1).

As a simple consequence of the LO NRQCD prediction, there should exist a 77% rule in the hadronic decay of the Υ

[5]The unnaturally small single-photon amplitude in this channel is due to the accidental suppression factor received by $c_{1,0}^{1}$, as can be seen in (13b).

[6]Note this situation is quite different from the continuum production process $e^+e^- \to J/\psi(\lambda) + \chi_{c2}(\tilde{\lambda})$, where the (0, 0) and $(\pm 1, 0)$ channels make the dominant contributions to the unpolarized production cross section [32].

[7]It is interesting to compare the relative importance of the various exclusive production channels $J/\psi + \chi_{cJ}$ ($J = 0, 1, 2$) in Υ decay and continuum production. For $e^+e^- \to J/\psi + \chi_{c0,1,2}$, one finds that the production rate for $J/\psi + \chi_{c0}$ is about one order of magnitude greater than those for $J/\psi + \chi_{c1,2}$ [31,32].

TABLE III. The unpolarized partial decay widths and the corresponding branching fractions that incorporate all three distinct decay mechanisms. The superscript $[J]$ characterizes the corresponding decay process $\Upsilon(1S, 2S, 3S) \to J/\psi + \chi_{cJ}$ $(J = 0, 1, 2)$.

	$\Gamma^{[0]}$ (eV)	$\mathcal{B}^{[0]}$	$\Gamma^{[1]}$ (eV)	$\mathcal{B}^{[1]}$	$\Gamma^{[2]}$ (eV)	$\mathcal{B}^{[2]}$
$\Upsilon(1S)$	0.070	1.3×10^{-6}	0.26	4.9×10^{-6}	0.011	2.0×10^{-7}
$\Upsilon(2S)$	0.035	1.1×10^{-6}	0.13	4.1×10^{-6}	0.0054	1.7×10^{-7}
$\Upsilon(3S)$	0.026	8.6×10^{-7}	0.099	3.3×10^{-6}	0.0041	1.3×10^{-7}

system, in analogy with the famous 12% rule in the ψ system,

$$\frac{\mathcal{B}[\Upsilon(2S) \to \text{hadrons}]}{\mathcal{B}[\Upsilon(1S) \to \text{hadrons}]} = \frac{\mathcal{B}[\Upsilon(2S) \to e^+e^-]}{\mathcal{B}[\Upsilon(1S) \to e^+e^-]} = 0.77 \pm 0.07. \quad (19)$$

Not surprisingly, the ratios of $\mathcal{B}[\Upsilon(2S) \to J/\psi + \chi_{cJ}]$ to $\mathcal{B}[\Upsilon(1S) \to J/\psi + \chi_{cJ}]$ in Table III are indeed compatible with this rule.

Thus far, the BELLE experiment has collected about 102 million $\Upsilon(1S)$ samples and 158 million $\Upsilon(2S)$ samples. According to Table III, the BELLE experiment is expected to have produced about 130 and 170 $\Upsilon(1S, 2S) \to J/\psi + \chi_{c0}$ events, 500 and 650 $\Upsilon(1S, 2S) \to J/\psi + \chi_{c1}$ events, 20 and 30 $\Upsilon(1S, 2S) \to J/\psi + \chi_{c2}$ events, respectively.

Experimentally, there are two possible methods to detect the $J/\psi + \chi_{c0,1,2}$ signals. The first is to reconstruct both the J/ψ and $\chi_{c0,1,2}$ events. The clean and copious decay modes of $\chi_{c1,2}$ are the $E1$ radiative transitions $\chi_{c1,2} \to J/\psi + \gamma$, with the branching fractions of 34.4% and 19.5%, respectively [1]. The J/ψ meson can be most cleanly tagged through the leptonic decays into e^+e^- and $\mu^+\mu^-$, with combined branching ratios about 12% [1]. Although this method has the advantage of bearing very low background level, taking into account the reconstruction efficiencies for two J/ψ and one photon, one may end up with too few signal events to be practically useful.

The second method is to only reconstruct one $J/\psi \to l^+l^-$ event, then fit the recoil mass spectrum against the J/ψ to estimate the number of $\chi_{c0,1,2}$ peak events. This method will not depend on the concrete decay modes of $\chi_{c0,1,2}$. For low statistics of signal events like in our case, this method is much more superior to the preceding one. As a matter of fact, this method has already been used by the BELLE collaboration to impose the upper bound for the exclusive bottomonium decays $\chi_{b0,1,2} \to J/\psi J/\psi, J/\psi\psi'$ [54].

In fitting the recoil mass spectrum of J/ψ, the net detection efficiency for $\Upsilon(1S, 2S) \to J/\psi + \chi_{c0,1,2}$ is estimated to be around 4% (similar for all $\chi_{c0,1,2}$), with the reconstruction efficiency for $J/\psi \to l^+l^-$ included [55]. Therefore, the numbers of the observed $\Upsilon(1S, 2S) \to J/\psi + \chi_{c1}$ events are expected to be $500 \times 4\% = 20$, and $650 \times 4\% = 26$, respectively. Since only one J/ψ is reconstructed, the background level in real data may not be very low. With only 20 reconstructed signal events, it seems quite challenging for the signal significance to reach the 5σ level, and a larger data pool is needed in order to draw a definite conclusion. In the prospective Super B factory, with a luminosity 50 times greater than the current B factory, it seems very promising that the decays $\Upsilon(1S, 2S, 3S) \to J/\psi + \chi_{c0,1}$ will be eventually observed.[8]

V. SUMMARY

In this paper, we carry out a comprehensive investigation on the exclusive $J/\psi + \chi_{c0,1,2}$ production in Υ decay in the NRQCD factorization framework. We have explicitly considered three distinct decay mechanisms, i.e., the strong, electromagnetic and radiative decay channels. Although there has not yet appeared a rigorous proof on the validity of NRQCD factorization approach to these types of double-charmonium production processes, the explicit verification for the cancelation of IR divergences in our calculation is rather supportive of the positive answer. Moreover, our explicit calculation further supports the previous claim that the double logarithms appearing in the one-loop NRQCD short-distance coefficients are always affiliated with the helicity-suppressed channels [32,50].

The branching fractions for the various polarized and unpolarized decay channels $\Upsilon(nS) \to J/\psi + \chi_{c0,1,2}$ $(n = 1, 2, 3)$ are predicted by incorporating all three distinct decay channels at the lowest order. In our case, the relative phase among these decay channels arise from the short-distance loop effect, which can actually be calculated in perturbation theory. There appears no universal interference pattern, but the three-gluon and the single-photon amplitudes often tend to be destructive. We find

[8]The partial widths of the similar decay processes $\Upsilon(1S, 2S, 3S) \to J/\psi + \chi'_{cJ}$, $\psi' + \chi_{cJ}$, $\psi' + \chi'_{cJ}$ $(J = 0, 1, 2)$ can also be readily obtained, provided that we substitute the appropriate kinematical factor and the corresponding (first derivative of) wave functions at the origin for ψ' and χ'_{cJ} in (11). Interestingly, the NRQCD formalism seems to imply that $\Upsilon \to J/\psi + \chi'_{cJ}$ may even have the greater decay rates than $\Upsilon \to J/\psi + \chi_{cJ}$, since $|R'_{\chi'_{cJ}}(0)| > |R'_{\chi_{cJ}}(0)|$ according to Ref. [52].

that $\Upsilon(nS)$ decays into $J/\psi + \chi_{c1}$ have the largest branching fraction, about a few times 10^{-6}; and the decays $\Upsilon(nS) \to J/\psi + \chi_{c2}$ have the smallest decay branching ratio, only of order 10^{-7}. The current statistics at BELLE is on the margin of observing these decay channels. If the prospective high-luminosity e^+e^- facilities such as the Super B experiment can dedicate more machine time on the first three Υ resonances, it should be an ideal place to discover their exclusive decay modes into $J/\psi + \chi_{c0,1}$.

ACKNOWLEDGMENTS

We are grateful to Cheng-Ping Shen and Chang-Zheng Yuan for the nice explanations of the experimental issues about detecting the $J/\psi + \chi_{cJ}$ signals in the BELLE experiment. This research was supported in part by the National Natural Science Foundation of China under Grants No. 10875130, No. 10875156, No. 10935012, No. 11125525, the DFG and NSFC (CRC 110), and by the Ministry of Science and Technology of China under Contract No. 2009CB825200 and China Postdoctoral Science Foundation Grant No. 2013M530733.

APPENDIX: VARIOUS HELICITY PROJECTORS FOR $\Upsilon \to J/\psi + \chi_{c0,1,2}$

During this work, we have utilized the various helicity projectors to expedite projecting out the corresponding helicity amplitudes associated with $\Upsilon \to J/\psi + \chi_{c0,1,2}$. This helicity projection technique, which has already been utilized in our previous work on the $\mathcal{O}(\alpha_s)$ correction to the process $\gamma^* \to J/\psi + \chi_{c0,1,2}$ [32], can significantly reduce the amount of labors required for the loop diagram calculations. In this Appendix, we collect the explicit formulas for the 10 helicity projectors used in this work.

First, it is convenient to introduce the transverse metric tensor

$$\begin{aligned} g_{\perp\mu\nu} &\equiv g_{\mu\nu} + \frac{P_\mu P_\nu}{|\mathbf{P}|^2} - \frac{Q\cdot P}{M_\Upsilon^2|\mathbf{P}|^2}(P_\mu Q_\nu + Q_\mu P_\nu) \\ &\quad + \frac{M_{J/\psi}^2}{M_\Upsilon^2}\frac{Q_\mu Q_\nu}{|\mathbf{P}|^2} \\ &= g_{\mu\nu} + \frac{\tilde{P}_\mu \tilde{P}_\nu}{|\mathbf{P}|^2} - \frac{Q\cdot \tilde{P}}{M_\Upsilon^2|\mathbf{P}|^2}(\tilde{P}_\mu Q_\nu + Q_\mu \tilde{P}_\nu) \\ &\quad + \frac{M_{\chi_{cJ}}^2}{M_\Upsilon^2}\frac{Q_\mu Q_\nu}{|\mathbf{P}|^2}, \end{aligned} \tag{A1}$$

where Q, P, and $\tilde{P}$ stand for the four-momenta of Υ, J/ψ, and χ_{cJ}, respectively. This symmetric tensor satisfies the transversity condition $g_{\perp\mu\nu}P^\mu = g_{\perp\mu\nu}\tilde{P}^\mu = 0$. It further has the properties $g_{\perp\mu}^{\mu} = 2$, $g_{\perp\mu\alpha}g_\perp^{\alpha\nu} = g_{\perp\mu\alpha}g^{\alpha\nu} = g_{\perp\mu}^{\nu}$.

The decay amplitude $\mathcal{A}^0$ for the process $\Upsilon \to J/\psi + \chi_{c0}$ can be parametrized as $\mathcal{A}^0 = \mathcal{A}^0_{\mu\nu}\epsilon_\Upsilon^\mu \epsilon_{J/\psi}^{*\nu}(\lambda)$, where ϵ_Υ and $\epsilon_{J/\psi}$ denote the polarization vectors of Υ and J/ψ, respectively. The helicities of J/ψ and χ_{c0} are labeled by λ and $\tilde{\lambda}$ (trivially $\tilde{\lambda} = 0$). There are only two independent helicity amplitudes for this process, which can be deduced by having the corresponding helicity projectors act on the amputated amplitude, $\mathcal{A}^0_{\lambda,\tilde{\lambda}} = \mathbb{P}^{\mu\nu}_{\lambda,\tilde{\lambda}}\mathcal{A}^0_{\mu\nu}$, up to an immaterial phase. The two helicity projection tensors for $\Upsilon \to J/\psi + \chi_{c0}$ are

$$\mathbb{P}^{\mu\nu}_{0,0} = \frac{1}{|\mathbf{P}|^2}\left(P_\mu - \frac{Q\cdot P}{M_\Upsilon^2}Q_\mu\right)\left(\frac{Q\cdot P}{M_{J/\psi}M_\Upsilon}P_\nu - \frac{M_{J/\psi}}{M_\Upsilon}Q_\nu\right), \tag{A2a}$$

$$\mathbb{P}^{\mu\nu}_{1,0} = -\frac{1}{2}g_{\perp\mu\nu}, \tag{A2b}$$

where $g_{\perp\mu\nu}$ is defined in (A1). These two projectors are normalized as $\mathbb{P}_{0,0;\mu\nu}\mathbb{P}^{\mu\nu}_{0,0} = 1$, $\mathbb{P}_{1,0;\mu\nu}\mathbb{P}^{\mu\nu}_{1,0} = \frac{1}{2}$ and orthogonal to each other, $\mathbb{P}_{0,0;\mu\nu}\mathbb{P}^{\mu\nu}_{1,0} = 0$.

The decay amplitude $\mathcal{A}^1$ for the decay process $\Upsilon \to J/\psi + \chi_{c1}$ can be expressed as $\mathcal{A}^1 = \mathcal{A}^1_{\mu\nu\alpha}\epsilon_\Upsilon^\mu \epsilon_{J/\psi}^{*\nu}(\lambda)\epsilon_{\chi_{c1}}^{*\alpha}(\tilde{\lambda})$, where $\tilde{\lambda}$ and $\epsilon_{\chi_{c1}}$ denote the helicity of the χ_{c1} state and the corresponding polarization vector. There are three independent helicity amplitudes for this process, which can be deduced by having the corresponding helicity projectors act on the amputated amplitude, $\mathcal{A}^1_{\lambda,\tilde{\lambda}} = \mathbb{P}^{\mu\nu\alpha}_{\lambda,\tilde{\lambda}}\mathcal{A}^1_{\mu\nu\alpha}$. The three helicity projection tensors for $\Upsilon \to J/\psi + \chi_{c1}$ read

$$\mathbb{P}^{\mu\nu\alpha}_{1,0} = \frac{i}{2M_\Upsilon|\mathbf{P}|^2}\epsilon_{\mu\nu\rho\sigma}Q^\rho \tilde{P}^\sigma\left(\frac{Q\cdot\tilde{P}}{M_{\chi_{c1}}M_\Upsilon}\tilde{P}_\alpha - \frac{M_{\chi_{c1}}}{M_\Upsilon}Q_\alpha\right), \tag{A3a}$$

$$\mathbb{P}^{\mu\nu\alpha}_{0,1} = -\frac{i}{2M_\Upsilon|\mathbf{P}|^2}\epsilon_{\mu\alpha\rho\sigma}Q^\rho P^\sigma\left(\frac{Q\cdot P}{M_{J/\psi}M_\Upsilon}P_\nu - \frac{M_{J/\psi}}{M_\Upsilon}Q_\nu\right), \tag{A3b}$$

$$\mathbb{P}^{\mu\nu\alpha}_{1,1} = \frac{i}{2M_\Upsilon|\mathbf{P}|^2}\epsilon_{\nu\alpha\rho\sigma}Q^\rho P^\sigma\left(P_\mu - \frac{Q\cdot P}{M_\Upsilon^2}Q_\mu\right), \tag{A3c}$$

which are subject to the normalization conditions $\mathbb{P}_{i;\mu\nu\alpha}\mathbb{P}^{\mu\nu\alpha}_{j} = \frac{1}{2}\delta_{ij}$, with i, j signifying one of the three helicity configurations.

Similarly, for the decay process $\Upsilon \to J/\psi + \chi_{c2}$, we can identify the amputated amplitude through $\mathcal{A}^2 = \mathcal{A}^2_{\mu\nu\alpha\beta}\epsilon_\Upsilon^\mu \epsilon_{J/\psi}^{*\nu}(\lambda)e_{\chi_{c2}}^{*\alpha\beta}(\tilde{\lambda})$, where $\tilde{\lambda}$ and $e_{\chi_{c2}}$ represent the helicity of the χ_{c2} state and the corresponding polarization tensor. There are in total five independent helicity amplitudes, which can be obtained by having the corresponding helicity projectors act upon the amputated amplitude, $\mathcal{A}^2_{\lambda,\tilde{\lambda}} = \mathbb{P}^{\mu\nu\alpha\beta}_{\lambda,\tilde{\lambda}}\mathcal{A}^2_{\mu\nu\alpha\beta}$. We construct the five helicity projection tensors for $\Upsilon \to J/\psi + \chi_{c2}$ as

$$\mathbb{P}_{0,0}^{\mu\nu\alpha\beta} = \frac{1}{\sqrt{6}|\mathbf{P}|^2}\left(\frac{Q\cdot P}{M_{J/\psi}M_\Upsilon}P_\nu - \frac{M_{J/\psi}}{M_\Upsilon}Q_\nu\right)\left(P_\mu - \frac{Q\cdot P}{M_\Upsilon^2}Q_\mu\right) \times\left[g_{\perp\alpha\beta} + \frac{2}{|\mathbf{P}|^2}\left(\frac{Q\cdot\tilde{P}}{M_{\chi_{c2}}M_\Upsilon}\tilde{P}_\alpha - \frac{M_{\chi_{c2}}}{M_\Upsilon}Q_\alpha\right)\left(\frac{Q\cdot\tilde{P}}{M_{\chi_{c2}}M_\Upsilon}\tilde{P}_\beta - \frac{M_{\chi_{c2}}}{M_\Upsilon}Q_\beta\right)\right], \tag{A4a}$$

$$\mathbb{P}_{1,0}^{\mu\nu\alpha\beta} = -\frac{1}{2\sqrt{6}}g_{\perp\mu\nu}\left[g_{\perp\alpha\beta} + \frac{2}{|\mathbf{P}|^2}\left(\frac{Q\cdot\tilde{P}}{M_{\chi_{c2}}M_\Upsilon}\tilde{P}_\alpha - \frac{M_{\chi_{c2}}}{M_\Upsilon}Q_\alpha\right)\left(\frac{Q\cdot\tilde{P}}{M_{\chi_{c2}}M_\Upsilon}\tilde{P}_\beta - \frac{M_{\chi_{c2}}}{M_\Upsilon}Q_\beta\right)\right], \tag{A4b}$$

$$\mathbb{P}_{0,1}^{\mu\nu\alpha\beta} = \frac{1}{2\sqrt{2}|\mathbf{P}|^2}\left(\frac{Q\cdot P}{M_{J/\psi}M_\Upsilon}P_\nu - \frac{M_{J/\psi}}{M_\Upsilon}Q_\nu\right)\left[g_{\perp\mu\alpha}\left(\frac{Q\cdot\tilde{P}}{M_{\chi_{c2}}M_\Upsilon}\tilde{P}_\beta - \frac{M_{\chi_{c2}}}{M_\Upsilon}Q_\beta\right) + (\alpha\leftrightarrow\beta)\right], \tag{A4c}$$

$$\mathbb{P}_{1,1}^{\mu\nu\alpha\beta} = -\frac{1}{2\sqrt{2}|\mathbf{P}|^2}\left(P_\mu - \frac{Q\cdot P}{M_\Upsilon^2}Q_\mu\right)\left[g_{\perp\nu\alpha}\left(\frac{Q\cdot\tilde{P}}{M_{\chi_{c2}}M_\Upsilon}\tilde{P}_\beta - \frac{M_{\chi_{c2}}}{M_\Upsilon}Q_\beta\right) + (\alpha\leftrightarrow\beta)\right], \tag{A4d}$$

$$\mathbb{P}_{1,2}^{\mu\nu\alpha\beta} = \frac{1}{4}(g_{\perp\mu\nu}g_{\perp\alpha\beta} - g_{\perp\mu\alpha}g_{\perp\nu\beta} - g_{\perp\mu\beta}g_{\perp\nu\alpha}). \tag{A4e}$$

These five projection operators satisfy the normalization conditions $\mathbb{P}_{i;\mu\nu\alpha\beta}\mathbb{P}_{j;}^{\mu\nu\alpha\beta} = \frac{1}{2}\delta_{ij}$ (i, j corresponding to one of the five helicity configurations), except that $\mathbb{P}_{0,0;\mu\nu\alpha\beta}\mathbb{P}_{0,0}^{\mu\nu\alpha\beta} = 1$.

All the helicity projectors are derived by obeying the exact decay kinematics. Nevertheless, in this work we only target at the LO accuracy in v expansion. Therefore, upon applying these projectors to infer the intended helicity amplitudes, it is eligible to make the following substitutions for the various quarkonium masses: $M_{\Upsilon(nS)} \approx 2m_b$ ($n = 1, 2, 3$), and $M_{J/\psi} \approx M_{\chi_{c0,1,2}} \approx 2m_c$. Implementing these approximations considerably simplifies the corresponding loop calculation.

[1] J. Beringer *et al.* (Particle Data Group Collaboration), Phys. Rev. D **86**, 010001 (2012).
[2] C. P. Shen *et al.* (Belle Collaboration), Phys. Rev. D **86**, 031102 (2012).
[3] Y. Jia, Phys. Rev. D **78**, 054003 (2008).
[4] B. Gong, Y. Jia, and J. X. Wang, Phys. Lett. B **670**, 350 (2009).
[5] V. V. Braguta and V. G. Kartvelishvili, Phys. Rev. D **81**, 014012 (2010).
[6] P. Sun, G. Hao, and C. F. Qiao, Phys. Lett. B **702**, 49 (2011).
[7] V. V. Braguta, A. K. Likhoded, and A. V. Luchinsky, Phys. Rev. D **72**, 094018 (2005).
[8] V. V. Braguta, A. K. Likhoded, and A. V. Luchinsky, Phys. Rev. D **80**, 094008 (2009); **85**, 119901(E) (2012).
[9] J. Zhang, H. Dong, and F. Feng, Phys. Rev. D **84**, 094031 (2011).
[10] W.-L. Sang, R. Rashidin, U.-R. Kim, and J. Lee, Phys. Rev. D **84**, 074026 (2011).
[11] L.-B. Chen and C.-F. Qiao, J. High Energy Phys. 11 (2012) 168.
[12] B. A. Irwin, B. Margolis, and H. D. Trottier, Phys. Rev. D **42**, 1577 (1990).
[13] Y. Jia, Phys. Rev. D **76**, 074007 (2007).
[14] K. Abe *et al.* (Belle Collaboration), Phys. Rev. Lett. **89**, 142001 (2002).
[15] K. Abe *et al.* (Belle Collaboration), Phys. Rev. D **70**, 071102 (2004).
[16] B. Aubert *et al.* (*BABAR* Collaboration), Phys. Rev. D **72**, 031101 (2005).
[17] E. Braaten and J. Lee, Phys. Rev. D **67**, 054007 (2003).
[18] K. Y. Liu, Z. G. He, and K. T. Chao, Phys. Lett. B **557**, 45 (2003).
[19] K. Hagiwara, E. Kou, and C. F. Qiao, Phys. Lett. B **570**, 39 (2003).
[20] J. P. Ma and Z. G. Si, Phys. Rev. D **70**, 074007 (2004).
[21] A. E. Bondar and V. L. Chernyak, Phys. Lett. B **612**, 215 (2005).
[22] G. T. Bodwin, D. Kang, and J. Lee, Phys. Rev. D **74**, 114028 (2006).
[23] Y.-J. Zhang, Y.-j. Gao, and K.-T. Chao, Phys. Rev. Lett. **96**, 092001 (2006).
[24] B. Gong and J. X. Wang, Phys. Rev. D **77**, 054028 (2008).
[25] Z. G. He, Y. Fan, and K. T. Chao, Phys. Rev. D **75**, 074011 (2007).
[26] G. T. Bodwin, J. Lee, and C. Yu, Phys. Rev. D **77**, 094018 (2008).
[27] V. V. Braguta, Phys. Rev. D **79**, 074018 (2009).
[28] For a recent review on $e^+e^- \to J/\psi + \eta_c$ at B factory, see N. Brambilla *et al.*, Eur. Phys. J. C **71**, 1534 (2011).
[29] H.-R. Dong, F. Feng, and Y. Jia, Phys. Rev. D **85**, 114018 (2012).
[30] Y.-J. Zhang, Y.-Q. Ma, and K.-T. Chao, Phys. Rev. D **78**, 054006 (2008).
[31] K. Wang, Y.-Q. Ma, and K.-T. Chao, Phys. Rev. D **84**, 034022 (2011).
[32] H.-R. Dong, F. Feng, and Y. Jia, J. High Energy Phys. 10 (2011) 141; 02 (2013) 089(E).
[33] G. T. Bodwin, E. Braaten, and G. P. Lepage, Phys. Rev. D **51**, 1125 (1995); **55**, 5853(E) (1997).
[34] J. Xu, Ph.D. thesis, IHEP, 2011 (in Chinese).

[35] G. Lopez Castro, J. L. Lucio M and J. Pestieau, AIP Conf. Proc. **342**, 441 (1995).
[36] R. Baldini *et al.*, Phys. Lett. B **444**, 111 (1998).
[37] M. Suzuki, Phys. Rev. D **60**, 051501 (1999).
[38] P. Wang, C. Z. Yuan, and X. H. Mo, Phys. Rev. D **69**, 057502 (2004).
[39] C. Z. Yuan, P. Wang, and X. H. Mo, Phys. Lett. B **567**, 73 (2003).
[40] S. Dobbs *et al.* (CLEO Collaboration), Phys. Rev. D **74**, 011105 (2006).
[41] M. Jacob and G. C. Wick, Ann. Phys. (Berlin) **7**, 404 (1959); **281**, 774 (2000).
[42] H. E. Haber, arXiv:hep-ph/9405376.
[43] S. J. Brodsky and G. P. Lepage, Phys. Rev. D **24**, 2848 (1981).
[44] G. P. Lepage and S. J. Brodsky, Phys. Rev. D **22**, 2157 (1980).
[45] V. L. Chernyak and A. R. Zhitnitsky, Phys. Rep. **112**, 173 (1984).
[46] G. T. Bodwin, X. Garcia i Tormo, and J. Lee, Phys. Rev. Lett. **101**, 102002 (2008).
[47] T. Hahn and M. Perez-Victoria, Comput. Phys. Commun. **118**, 153 (1999).
[48] A. V. Smirnov, J. High Energy Phys. 10 (2008) 107.
[49] F. Feng, Comput. Phys. Commun. **183**, 2158 (2012).
[50] Y. Jia, J. X. Wang, and D. Yang, J. High Energy Phys. 10 (2011) 105.
[51] R. K. Ellis and G. Zanderighi, J. High Energy Phys. 02 (2008) 002. Also see the website http://qcdloop.fnal.gov.
[52] E. J. Eichten and C. Quigg, Phys. Rev. D **52**, 1726 (1995).
[53] J. M. Gerard and J. Weyers, Phys. Lett. B **462**, 324 (1999).
[54] C. P. Shen *et al.* (Belle Collaboration), Phys. Rev. D **85**, 071102 (2012).
[55] C. P. Shen (private communication).